

# Determination of the Optimal Bacteriophage Dose to Control *Pseudomonas aeruginosa* using evolutionary programming and stochastic kinetics

Diana C Ardila <sup>1</sup>, Juan D Castro <sup>1</sup>, Angela V Holguín <sup>2</sup>, Viviana Clavijo <sup>2</sup>, Catalina Prada <sup>2</sup>, Martha J Vives <sup>2</sup>, Andres F Andres Gonzalez Barrios <sup>Corresp. 1</sup>

<sup>1</sup> Department of Chemical Engineering, Universidad de Los Andes, Bogota, CUNDINAMARCA, Colombia

<sup>2</sup> Department of Biological Sciences, Universidad de Los Andes, Bogota, CUNDINAMARCA, Colombia

Corresponding Author: Andres F Andres Gonzalez Barrios  
Email address: andgonza@uniandes.edu.co

Phage-therapy is a promising alternative against pathogenic, multiple drug resistant bacteria. In this work we propose an algorithm to determine the optimal bacteriophage dose able to minimize a population of *Pseudomonas aeruginosa*. Reverse engineering was used to determine the kinetic parameters; subsequently, a bi-level optimization platform was implemented for a model based on evolutionary programming. Our prediction of optimal dose was tested *in vitro* with planktonic cultures of *P. aeruginosa*. From the data obtained, we conclude that reverse engineering and stochastic simulations are a useful approach to find optimal phage doses against pathogenic bacteria, an important step for the implementation of phage-therapy.

1 **Determination of the Optimal Bacteriophage Dose to Control *Pseudomonas***  
2 ***aeruginosa* using evolutionary programming and stochastic kinetics**

3  
4 Diana Catalina Ardila<sup>1</sup>, Juan David Castro<sup>1</sup>, Ángela Victoria Holguín<sup>2</sup>, Viviana  
5 Clavijo<sup>2</sup>, Catalina Prada<sup>2</sup>, Martha Josefina Vives<sup>2</sup> and Andrés Fernando González-Barrios<sup>1\*</sup>

- 6  
7 1. Department of Chemical Engineering, Carrera 1E N 19 A - 40, Universidad de los Andes,  
8 Bogotá, Colombia. Tel (571) 3394949  
9 2. Department of Biological Sciences, Universidad de los Andes, Carrera 1E N 18A- 10,  
10 Bogotá, Colombia. Tel (571) 3394949

## 19 ABSTRACT

20 Phage-therapy is a promising alternative against pathogenic, multiple drug resistant bacteria. In  
21 this work we propose an algorithm to determine the optimal bacteriophage dose able to minimize  
22 a population of *Pseudomonas aeruginosa*. Reverse engineering was used to determine the kinetic  
23 parameters; subsequently, a bi-level optimization platform was implemented for a model based  
24 on evolutionary programming. Our prediction of optimal dose was tested *in vitro* with planktonic  
25 cultures of *P. aeruginosa*. From the data obtained, we conclude that reverse engineering and  
26 stochastic simulations are a useful approach to find optimal phage doses against pathogenic  
27 bacteria, an important step for the implementation of phage-therapy.

28

29

30 *Keywords:* Mathematical modeling, Phage-therapy, Optimal dose, *Pseudomonas aeruginosa*,

31

32

33

34

35

36

37

## 38 1. INTRODUCTION

39 The treatment of intra-hospital infections (nosocomial infections) has turned out to be an  
40 enormous challenge as the current microorganisms display high capability to resist multiple  
41 varieties of antibiotics. A number of bacterial resistance mechanisms against antibiotics exist

42 with some examples including: diffusional limitation provided by an exopolysaccharide matrix  
43 from biofilm assembly,<sup>[1]</sup> active site mutations where an antibiotic is no longer capable of  
44 binding to the cell wall and toxic molecule ejection through efflux pumps and transmembrane  
45 proteins,<sup>[2]</sup> among others.

46 Hospitals and more specifically Intensive Care Units are generally considered epicenters of  
47 antibiotic resistance and the principal sources of outbreaks of multiple drug-resistant bacteria.<sup>[3]</sup>

48 For this reason, biomedical communities have been urged to investigate new anti-bacterial  
49 treatments such as the next generation drugs and therapies with improved spectrums against  
50 resistant microorganisms.<sup>[4]</sup> Approaches based on bacteriophages (or phages), known as phage-

51 therapy, constitute an interesting alternative due to the ease of isolating phages capable of  
52 targeting antibiotic resistant bacteria. Also, viruses evolve with their host allowing them to infect  
53 phage-resistant cells when they would appear. Regarding the diffusional obstacles, antibiotics in  
54 general have to overcome several hurdles due to the presence of exopolysaccharides when the  
55 biofilm phenotype is present; phages, on the other hand, are in theory capable of efficiently  
56 penetrating the biofilm so the infection would be deeply inhibited.<sup>[5]</sup> The mechanism exploited in

57 phage therapy is the obligatorily lytic life cycle when the viral particles recognize the bacterial  
58 cell surface, followed by reversible and irreversible binding and the injection of its DNA or RNA  
59 from phage capsid into the host. Once the phage genome has shut down, most of the host's  
60 proteins are amplified inside the cell using its host's molecular machinery and consequently viral  
61 progeny are formed. Finally, cell lysis occurs resulting in progeny exiting the cell and repeating a  
62 new infective cycle.<sup>[6]</sup> *P. aeruginosa* is one of the principal causes of acquired infections and  
63 mortality in hospitals.<sup>[7]</sup> This microorganism is highly adaptive, considered an opportunist  
64 nosocomial pathogen and constitutes a high risk microorganism because of its virulence and

65 resistance to most antibiotics currently available.<sup>[8]</sup> Moreover, it affects different organs and  
66 anatomical sites such as the upper respiratory tract, lungs, heart valves, urinary tract, surgical  
67 tract and open wounds.<sup>[7]</sup>

68 The advent of mathematical biology has allowed a greater understanding of the underpinnings of  
69 several biological events with important applications for disease control. In order to get a better  
70 comprehension of the dynamics of the infection process deterministic and stochastic modeling  
71 was applied to predict the behavior of the phages infecting a planktonic population of several  
72 bacterial species.<sup>[9-12]</sup> Deterministic approaches are commonly used and assume that the species  
73 in the system change continuously and deterministically over time and are based on ordinary  
74 differential equations (ODES). These models describe the dynamics of the system in terms of the  
75 species present, and parameters related with the rates of change in the concentration of these  
76 species.<sup>[12]</sup> From this approximation, it's possible to make an evaluation of the parameters that  
77 have an influence on the rate of the infective process (kinetic parameters). Stochastic models are  
78 based on random collisions among reacting species, making them useful to simulate or predict  
79 events in biological systems such as metabolic regulation systems and genetic networks. The  
80 stochastic approach allows modeling phage-host infection in which the effects of noise,  
81 variations, and uncertainty are reflected in the system dynamics.<sup>[13]</sup>

82 Once the dynamics of the infection are understood, the search space or feasible region can be  
83 predicted to find the optimum therapeutic dose that would allow for controlling the pathogen and  
84 mitigate the occurrence of phage-resistance.<sup>[14]</sup> To do so, it's necessary to establish an  
85 optimization algorithm with an efficient searching capacity, satisfactory robustness and low  
86 computational demand. Our group has prior experience with using Monte Carlo-based  
87 algorithms to find the global optimum and one such example was simulated annealing to find the

88 quencher dose in *P. aeruginosa* quorum sensing networks.<sup>[15]</sup> Contrary to deterministic  
89 optimization, most of stochastic methods are not gradient based so either stochastic or  
90 deterministic models can be used as a template to find the optimum.

91 Different authors have studied the bacteriophage-host dynamics from only one or the other of the  
92 two approaches. Cairns *et al.* studied *Campylobacter* and bacteriophage interactions using a  
93 kinetic model based on ODES.<sup>[16]</sup> Jain *et al* used five different deterministic models to evaluate  
94 the infection dynamics of phage MS2 in its host *Escherichia coli*.<sup>[12]</sup> Arkin *et al* used a stochastic  
95 kinetic analysis to investigate the mechanism that causes the lysis-lysogeny decision circuit of  
96 phage  $\lambda$  in *E. coli*.<sup>[10]</sup> In a more recent study, Bardina *et al* made a stochastic formulation to study  
97 bacteriophage treatments for infections.<sup>[17]</sup> All these works have been made to understand the  
98 dynamics of phage-bacteria systems and calculate the parameters that affect the specific case of  
99 study.

100 Here in this study we proposed and applied an optimization platform, based on deterministic and  
101 stochastic-derived models built from previous experimental data to find the optimal dosage able  
102 to diminish a *P. aeruginosa* population. The experimental validation of the predicted dose was  
103 performed in three different ways: First, elucidating the behavior *in vitro* of the infection process.  
104 Second, evaluating the extrapolable characteristic of the dose to other phage-bacteria systems.  
105 And third, corroborating the optimal value of the dose performing a challenge test.

106

## 107 **2. MATERIALS AND METHODS**

### 108 **2.1. *Microorganism, growth medium and experimental curves acquisition***

109 In this study, three *Pseudomonas aeruginosa* strains resistant to multiple antibiotics (named *P.*  
110 *aeruginosa* P1, P3 and P4, kindly donated by Dr. Claudia Echeverri from Hospital Federico

111 LLeras Acosta, Ibagué, Colombia) were used. The three strains were used to isolate lytic  
112 bacteriophages; among them, three were selected for the assays (named F1, F2 and F3)  
113 (unpublished results). Bacterial strains were conserved by ultra-low freezing at  $-80^{\circ}\text{C}$  in 10%  
114 glycerol. Bacteriophages were maintained in Salt Medium buffer, SM (Composition: 0.05 mol/L  
115 of Tris-HCl pH 7.5,  $0.1\text{ mol L}^{-1}$  of NaCl,  $10\text{ mol/m}^3$   $\text{MgSO}_4$ , gelatin at 1% w/v) at  $4^{\circ}\text{C}$ .

116 In order to establish the bacterial growth kinetics, two different sets of experiments were done in  
117 triplicate; first, individual growth curves for strains of *P. aeruginosa* P1, P3 and P4 were  
118 performed. Each strain was inoculated in  $3\text{ cm}^3$  of minimal salt medium (MSM) (composition per  
119 liter:  $\text{KH}_2\text{PO}_4$  3.5 g,  $(\text{NH}_4)_2\text{HPO}_4$  1.0 g,  $\text{MgSO}_4$  1.2 g, glucose 5.0 g, trace elements solution 12.0  
120  $\text{cm}^3$ ; trace elements solution composition per liter: iron citrate III 60 mg, EDTA III 8.4 mg,  
121  $\text{CoCl}_2 \cdot 6\text{H}_2\text{O}$  2.76 mg,  $\text{MnCl}_2 \cdot 4\text{H}_2\text{O}$  15 mg, zinc acetate 8.4 mg,  $\text{Na}_2\text{MoO}_4 \cdot 2\text{H}_2\text{O}$  2.67 mg,  $\text{H}_3\text{BO}_3$   
122 3.3 mg,  $\text{CuCl}_2 \cdot 2\text{H}_2\text{O}$  1.5 mg). Cultures were grown overnight at 200 rpm and  $37^{\circ}\text{C}$ . Three  
123 hundred  $\mu\text{l}$  of the overnight culture was transferred to  $30\text{ cm}^3$  of MSM; these day cultures were  
124 incubated for 20 hours at 200 rpm and  $37^{\circ}\text{C}$ . Then,  $3\text{ cm}^3$  of the day cultures were transferred to  
125  $30\text{ cm}^3$  of MSM and were incubated at  $37^{\circ}\text{C}$  and 200 rpm, and for the duration of 18 hours  
126 optical density, colony forming units per cubic centimeter ( $\text{CFU/cm}^3$ ) and glucose concentrations  
127 (*BioSystems*<sup>®</sup> glucose kit) were measured. This data corresponds to what is will now be referred  
128 to as uninfected cultures. Second, to determine the effect of bacteriophages on the bacterial  
129 strains, each strain was grown as described above to the logarithmic phase; then,  $200\text{ }\mu\text{l}$  of phage  
130 F1 at a concentration of  $10^5\text{ PFU/cm}^3$  approximately (PFU, plaque forming units), was added to  
131 the bacterial cultures. Cultures were followed for 18 hours in triplicate where the optical density,  
132 viable cell concentration and glucose concentration, as already described for the uninfected  
133 cultures, were measured.





153 the rate at which supernatant phage particles degrade,  $y_{x/s}$  is the yield factor relating production of  
 154 uninfected bacterial cells to substrate consumed,  $\mu_{max,x}$  is the maximal growth of uninfected cells,  
 155 and  $K_{s,x}$  is the Monod constant for uninfected cells. The uninfected cell density corresponds to  
 156 the counts of viable cells in culture, measured in CFU/cm<sup>3</sup>; the infected cell density is the  
 157 difference between the counts in CFU/cm<sup>3</sup> of the infected culture and those of uninfected  
 158 cultures (comparing a phage infected flask to a control flask). Free phage densities for the  
 159 different cultures were obtained based on the profiles provided during the solution of the set of  
 160 differential equations for each model.

161

162 *Model 2.* Here, moreover uninfected cells, infected cells display growth at the same rate. This  
 163 model is derived from Model 1.

164

$$165 \quad \frac{dx}{dt} = \mu_x x - k_1 Px - k_2 x \quad (6)$$

166

$$167 \quad \frac{dy}{dt} = \mu_x y + k_1 Px - k_3 y \quad (7)$$

168

$$169 \quad \frac{dP}{dt} = k_4 y - k_1 Px - k_5 P \quad (8)$$

170

$$171 \quad \frac{ds}{dt} = -\mu_x x \frac{1}{y_{x/s}} - \mu_x y \frac{1}{y_{x/s}} \quad (9)$$

172

173 
$$\mu_x = \frac{\mu_{\max,x}S}{K_{s,x} + S} \quad (10)$$

174 *Model 3.* In this model, uninfected and infected cells grow at different rates; equations derived  
 175 from this assumption follows:

176  
 177 
$$\frac{dx}{dt} = \mu_x x - k_1 Px - k_2 x \quad (11)$$

178  
 179  
 180 
$$\frac{dy}{dt} = \mu_y y + k_1 Px - k_3 y \quad (12)$$

181  
 182  
 183 
$$\frac{dP}{dt} = k_4 y - k_1 Px - k_5 P \quad (13)$$

184  
 185  
 186 
$$\frac{ds}{dt} = -\mu_x x \frac{1}{y_{x/s}} - \mu_y y \frac{1}{y_{y/s}} \quad (14)$$

187  
 188  
 189 
$$\mu_x = \frac{\mu_{\max,x}S}{K_{s,x} + S} \quad (15)$$

190  
 191  
 192 
$$\mu_y = \frac{\mu_{\max,y}S}{K_{s,y} + S} \quad (16)$$

193  
 194 Where  $\mu_y$  is the growth rate of infected cells,  $\mu_{\max,y}$  is the maximal growth rate of infected cells,  
 195  $K_{s,y}$  is the Monod constant for infected cells, and  $y_{y/s}$  is the yield factor relating production of  
 196 infected bacterial cells to substrate consumed.

197  
 198 *Model 4.* Here, only uninfected cells grow; and are split in two different populations: susceptible  
 199 to the phage (z), and resistant to the phage (R). Resistant cells display growth.

200  
 201 
$$\frac{dz}{dt} = \mu_z z - k_1 Pz - k_2 z \quad (17)$$

202

203

204

$$\frac{dR}{dt} = \mu_R R - k_6 R \quad (18)$$

205

206

207

$$\frac{dy}{dt} = k_1 Pz - k_3 y \quad (19)$$

208

209

210

$$\frac{dP}{dt} = k_4 y - k_1 Pz - k_5 P \quad (20)$$

211

212

213

$$\frac{ds}{dt} = -\mu_z z \frac{1}{y_{z/s}} - \mu_R R \frac{1}{y_{R/s}} \quad (21)$$

214

215

216

$$\mu_z = \frac{\mu_{\max,z} S}{K_{s,z} + S} \quad (22)$$

217

218

219

$$\mu_R = \frac{\mu_{\max,R} S}{K_{s,R} + S} \quad (23)$$

220

221

222

$$x = R + z \quad (24)$$

223

224

225 *Model 5.* In this model, only uninfected cells grow, and are split in two different populations:

226 susceptible to the phage ( $z$ ), and resistant to the phage. Resistant cells display growth. The lysis

227 of infected cells is unleashed after 480 min.

228

229

$$\frac{dz}{dt} = \mu_z z - k_1 Pz - k_2 z \quad (25)$$

230

$$231 \quad \frac{dR}{dt} = \mu_R R - k_6 R \quad (26)$$

232

$$233 \quad \frac{dy}{dt} = k_1 Pz - k_3 yU \quad (27)$$

234

$$235 \quad \frac{dP}{dt} = k_4 yU - k_1 Pz - k_5 P \quad (28)$$

236

$$237 \quad \frac{ds}{dt} = -\mu_z z \frac{1}{y_{z/s}} - \mu_R R \frac{1}{y_{R/s}} \quad (29)$$

238

$$239 \quad \mu_z = \frac{\mu_{\max,z} S}{K_{s,z} + S} \quad (30)$$

240

$$241 \quad \mu_R = \frac{\mu_{\max,R} S}{K_{s,R} + S} \quad (31)$$

242

$$243 \quad x = R + z \quad (32)$$

244

245 Where  $U$  is 0 when  $t \leq 480$  min and 1 when  $t > 480$  min.

246

247

248 *Model 6.* Finally, for model six, uninfected and infected cells grow at different rates; and lysis of  
 249 infected cells occurs after 480 min.

250

251 
$$\frac{dx}{dt} = \mu_x x - k_1 Px - k_2 x \quad (33)$$

252

253 
$$\frac{dy}{dt} = \mu_y y + k_1 Px - k_3 yU \quad (34)$$

254

255 
$$\frac{dP}{dt} = k_4 yU - k_1 Px - k_5 P \quad (35)$$

256

257 
$$\frac{ds}{dt} = -\mu_x x \frac{1}{y_{x/s}} - \mu_y y \frac{1}{y_{y/s}} \quad (36)$$

258

259 
$$\mu_x = \frac{\mu_{\max,x} S}{K_{s,x} + S} \quad (37)$$

260

261 
$$\mu_y = \frac{\mu_{\max,y} S}{K_{s,y} + S} \quad (38)$$

262

263

264 Simulated annealing and genetic algorithms were used to perform the parametric regression from  
 265 experimental data with an estimated phage dose of  $1 \times 10^5$  PFU/cm<sup>3</sup> using the System biology  
 266 toolbox in Matlab<sup>®</sup>.<sup>[18]</sup> Finally the three individual models that best described each system *in*  
 267 *vitro* (*P. aeruginosa* P1, P3 and P4 infected with phage F1) were merged to create a petri net  
 268 capable of describing the infection dynamics of F1 infecting these three strains in unison (Fig. 1).

269

### 270 **2.3. Determination of the optimal dose**

271 The optimization problem consisted of finding the optimum initial phage dose and the time in  
 272 which bacteria must be exposed to phages to minimize the population of each strain tested

273 (initial time of infection) using the global model built from each interaction analyzed. The  
 274 optimization problem can be posed as:

275

$$276 \quad \min_{t_i, x_{p1(0)}, x_{p3(0)}, x_{p4(0)}} PD \quad (34)$$

277

$$278 \quad s.t. 0.1 < x_{p1(t_i)}, x_{p3(t_i)}, x_{p4(t_i)} \quad (35)$$

279

280 where  $t_i$  is the time where the total bacterial population is minimized,  $x_{p1(0)}$ ,  $x_{p3(0)}$ ,  $x_{p4(0)}$  are the  
 281 initial conditions of living cells for each *P. aeruginosa* strain and  $x_{p1(t_i)}$ ,  $x_{p3(t_i)}$ ,  $x_{p4(t_i)}$  represent the  
 282 cell population for each strain at  $t_i$  and PD is the initial phage dose.

283

#### 284 **2.4. Stochastic modeling for optimal dose validation in silico**

285

286 We previously emphasized the need for validating the predicted dose in biological systems due  
 287 to the presence of uncertainty and variation. It is known that this noise could lead to the  
 288 appearance of dispersion in the population besides the objective function dispersion, so the dose  
 289 reported by our platform cannot represent the actual dose to eradicate the presence of the  
 290 pathogen.

291 To assess this, we performed stochastic simulations by numerically solving the master equation  
 292 based on the Gillespie algorithm. A review of the main features of the master equation formalism  
 293 and the Gillespie algorithm is given by Gillespie, 1977.<sup>[13]</sup> Briefly, the master equation is used to  
 294 describe the evolution of a system over time that can be in one particular state at a given time  
 295 point and then switch between states and be treated probabilistically. With the Gillespie

296 algorithm it's possible to simulate the temporal behavior of a system by calculating the  
297 probability of each discrete event occurring, and the resulting changes in the number of each  
298 species participating. For each simulation that was done, it gave a representative case of the  
299 timing and the sequence of events of phage infection in individual bacteria. In order to obtain  
300 statistical significance and a more accurate representation of the system multiple runs with the  
301 same initial conditions were done. For our purposes petri nets were derived from a merged  
302 deterministic model (Fig. 1) and one hundred thousand runs were performed with the optimum  
303 dose predicted by the genetic algorithm. For this, we deployed two different virtual clusters in  
304 three computer rooms with 35 computers each. All computers had an Intel Core 2 Duo 1.8 GHz  
305 processor and 4GBs of RAM. Virtual machines were assigned with both cores and 1 GB of  
306 RAM.

307

### 308 **2.5. Experimental validation of the optimal dose**

309

310 The predicted dose was experimentally validated *in vitro* in order to test the accuracy of the  
311 computational models. To achieve this, each strain was grown in MSM to logarithmic phase,  
312 established by the deterministic models: *P. aeruginosa* P1 was grown up to  $10^9$  CFU/cm<sup>3</sup>, *P.*  
313 *aeruginosa* P3 up to  $10^8$  CFU/cm<sup>3</sup>, *P. aeruginosa* P4 up to  $10^6$  CFU/cm<sup>3</sup>. At the desired cell  
314 density, each bacteriophage was added, separately, at a concentration of  $10^7$  PFU/cm<sup>3</sup>. The  
315 cultures were monitored for 1100 minutes where optical density and bacterial survivors were  
316 measured.

317 Additional tests were also performed with the P4 strain and the phage F1 to assess the potential  
318 difference in kinetics with varied phage doses above and below the optimal dose. P4 was grown  
319 in MSM to logarithmic phase, as described earlier, in two different cultures and the phage were

320 added at a final concentration of  $10^6$  PFU/cm<sup>3</sup> and  $10^8$  PFU/cm<sup>3</sup>, respectively. Cultures were  
321 monitored for 1100 min and optical densities and bacterial survivors were measured.

322 All the experiments explained in this section were carried out in triplicate.

323

324

### 325 **3. RESULTS AND ANALYSIS**

326

#### 327 **3.1. *Phage-strain individual models***

328

329 Models 1 through 6 were tested against experimental data using least squares sum, to determine

330 which assumptions described the dynamics best (Table 1). Interestingly, we found kinetic

331 parameters and model fitness were dependent on the strain analyzed. For *P. aeruginosa* P1 and

332 P3 infected with phage F1, the model that best described the infection process was Model 6. ,

333 Model 2 best described the infection process of *P. aeruginosa* P4 infected with phage F1

334 however. This is likely because *P. aeruginosa* P1 and P3 uninfected cells grew at different rates

335 (infected cells had a different growth rate since the number of infected cells is calculated as the

336 total cell population minus the uninfected cells), and a decline in the population of uninfected

337 cells of *P. aeruginosa* P4 wasn't observed (Fig. 2), meaning infected cells weren't as prevalent.

338 Model selection and parameterization is strongly influenced by the strain due to differences in

339 interaction dynamics, the mechanisms of infection and/or bacterial resistance to phage F1.

340 According to our data, P4 continues to grow as an uninfected culture, indicating that this strain

341 had weaker respond to phage F1 (Fig. 2). We believe that this difference is based on dissimilar

342 adsorption rates and parameters, DNA injection, DNA replication, progeny assembly, among

343 others, which were not taken into account in this case. We observed that the infection process is

344 also dependent on the length of the eclipse phase, which suggested that it was dependent on the

345 bacterial strain. For example, *P. aeruginosa* P3 displayed a clear lytic process after 1500 minutes



346 (Fig. 2B) whereas lysis in *P. aeruginosa* P1 took place in a shorter period of time (around 500  
347 minutes) (Fig. 2A). No lysis was observed with *P. aeruginosa* P4 and the cells continued to  
348 grow.

349 In Table 2 the kinetic parameters for each system shown in accordance with the model that best  
350 fit. These parameters were used later to feed the model for optimal dose calculations.

351 Additionally an indentifiability analysis of all six models was made using GenSSI, a Matlab  
352 toolbox for studying structural indentifiability using iterative lie derivatives and indentifiability  
353 tableaux.<sup>[19]</sup> With this analysis we could determine that models 1, 2, 3, 4, and 6 are globally  
354 indentifiable (results not shown), which means there is only one solution for the parameters of  
355 each model using our experimental data. The model five has two non-indentifiable parameters:  $k_2$   
356 and  $k_6$ . However, these parameters are easy to obtain directly from experimental data as is  
357 described in Jain et al, 2006. <sup>[12]</sup> Furthermore, this model didn't fit any of the experimental data  
358 and was not used for calculating the optimized phage dose.

359

### 360 **3.2. Optimal phage dose**

361 Evolutionary programming was used to calculate the optimum dose. This algorithm was chosen  
362 for a number of reasons including being less demanding of computational resources and its  
363 natural relation with biological systems, as it is based on Darwinian evolution. The system  
364 assumed the presence of the three *P. aeruginosa* strains, aiming to simulate a clinical infection  
365 caused by any one of the three strains. Genetic algorithm parameters were heuristically  
366 determined using a gene probability of 0.5 and a tolerance of 0.001. We initially obtained the  
367 model for each strain in order to elucidate the mechanism without considering the possible  
368 interactions among strains. Then, we fused them together and proposed a Petri net that represents

369 the communication between each model (Fig. 1). We obtained thirteen ordinary differential  
370 equations, which relate the initial population for each strain, the initial phage dose, and the length  
371 of infection. The differential equation system was used to feed kinetic parameters previously  
372 found and was coupled with the genetics algorithm platform and the optimal dose was evaluated.  
373 With a treatment time of 1,100 min the genetic algorithm predicted an optimal dose for the phage  
374 concentration of  $6.50 \times 10^7$  PFU/cm<sup>3</sup>. Numerical integration of the ordinary differential  
375 equations using the Runge Kutta fourth order method predicts that the bacterial survivors of *P.*  
376 *aeruginosa* P1 would decrease from  $1.2 \times 10^5$  to  $8.4 \times 10^2$  CFU/ cm<sup>3</sup>, *P. aeruginosa* P3 from  $5 \times$   
377  $10^8$  CFU/cm<sup>3</sup> to  $2 \times 10^3$  CFU/cm<sup>3</sup>, *P. aeruginosa* P4 from  $9 \times 10^6$  CFU/cm<sup>3</sup> to  $3 \times 10^3$  CFU/cm<sup>3</sup>  
378 (results not shown). The mixed population model (P1, P3, and P4) would be reduced from  $1.4 \times$   
379  $10^9$  CFU/cm<sup>3</sup> to  $2.16 \times 10^5$  CFU/cm<sup>3</sup> (Fig. 3).

380

### 381 **3.3. Phage dose stochastic validation**

382 Master equations of each biological system were numerically solved based on the Gillespie  
383 algorithm with a software, developed by our group, called Bacterium Simulator Grid.<sup>[20]</sup> 1,000  
384 simulations were performed aiming to obtain a representative sample and statistical distribution  
385 of the population. Due to a change in the scale (from macro-scale to micro-scale) it was  
386 mandatory to modify the initial conditions for each strain; resulting in 150 individuals being  
387 selected as the initial conditions for each strain. Optimal phage dose was also scaled to 430 free  
388 phage particles. Population histograms displayed a unimodal distribution of the population  
389 (results not shown) and an efficient action of the phage based on the small dispersion obtained  
390 (Standard deviation=  $\pm 5.12$  cells at time= 2,000 s). The host population decreased by an order of  
391 magnitude after an infection time of 2,000 s (equivalent to 33.33 min) (Fig. 4). Interestingly, we

392 found a positive correlation between the uninfected cells dispersion and time, suggesting that the  
393 viral inoculation should take place in early stages, similar to a prophylactic application, in order  
394 to avoid dispersion of the bacteria. The early presence of the phage would also lower the phage  
395 dose needed to eliminate the pathogen.

396

### 397 **3.4. Phage dose experimental validation**

398 In order to elucidate the behavior of the system *in vitro* using the optimum phage dose predicted  
399 infection curves were assayed. *P. aeruginosa* P1, P3, and P4 strains were grown as explained  
400 before and phage F1 was added in the optimum dose in early stages of bacterium growth based  
401 on our stochastic predictions. After 1,100 min, the bacterial survivors of all strains were reduced  
402 similarly to the predictions of our model. *P. aeruginosa* P1 cells decreased from  $2.95 \times 10^6$   
403 CFU/cm<sup>3</sup> to  $4.25 \times 10^3$  CFU/cm<sup>3</sup>, *P. aeruginosa* P3 decreased from  $1.17 \times 10^8$  CFU/cm<sup>3</sup> to  $2.1 \times$   
404  $10^3$  CFU/cm<sup>3</sup>, *P. aeruginosa* P4 from  $3.17 \times 10^7$  CFU/cm<sup>3</sup> to  $3.87 \times 10^2$  CFU/cm<sup>3</sup>. These results,  
405 as well as simulations, indicate that the phage is most effective against P3 strain and it is able to  
406 diminish populations of the other two strains. In Table 3 a comparison between simulation  
407 results and the experimental data with optimal dose is shown. The simulation results were  
408 corroborated and the optimum phage dose was validated; by using reverse engineering and  
409 utilizing stochastic simulations it is possible to find optimal phage doses against pathogenic  
410 bacteria. This optimization approach can help reduce wet laboratory trials, saving time and  
411 resources.

412 To test if the obtained optimal dose could be extrapolated to different phages, infection curves of  
413 P1, P3 and P4 were conduct using phages F2 and F3 (Results not shown). The total population  
414 reduction was calculated as the difference between the total population of the control curve

415 (uninfected) at 1100min and the total population of the infection curve at 1100 min (Table 4).  
416 Results showed that, with these phages when added to the culture at an optimal dose of  $6 \times 10^7$   
417 PFU/cm<sup>3</sup>, the population of all three *P. aeruginosa* strains was reduced by seven orders of  
418 magnitude or more.

419 To challenge the optimal dose we assayed two additional phage doses, one above and one below  
420 the optimal dose, using strain *P. aeruginosa* P4 and phage F1 (Fig. 5). With a phage dose of  $10^6$   
421 PFU/cm<sup>3</sup>, one log unit below the predicted optimal dose, the population of bacteria was reduced  
422 as expected. Similar behavior is also observed in infections using a phage dose one log unit  
423 above the optimal dose predicted ( $10^8$  PFU/cm<sup>3</sup>). In this scenario, our hypothesis pointed to a  
424 bigger reduction of bacteria population, or at least one obtained with the optimal dose.  
425 Nevertheless, the results indicate at the beginning of an infection a reduction of the bacteria  
426 population was experienced but at around 420 min phage-resistance occurred. It has been  
427 demonstrated in previous phage-host systems that a threshold exists where the overabundance of  
428 phage puts selective pressure on their host to resist them, in turn causing the phages to be  
429 ineffective.<sup>[21, 22, 23]</sup> This can be explained by different mechanisms: first, due the high number of  
430 viral particles, the capacity of them to be adsorbed on the bacteria surface is reduced.<sup>[21]</sup> As a  
431 consequence, the phage dies in the early stages of the infection process resulting in no viable  
432 phage progeny being assembled. This phenomenon is called lysis from without.<sup>[24]</sup> Second, at  
433 high PFU the bacteria can rapidly acquire certain resistance to the phages resulting in an abortive  
434 infection.<sup>[21]</sup> This phenomenon is due in part because using higher MOIs (MOI, multiplicity of  
435 infection) results in one generation of progeny being successfully produced which can result in a  
436 rapid development of resistance.<sup>[25]</sup> This resistance is caused by specific factors and avenues that

437 are required for productive phage infection being altered in such a way that inhibit phage-  
438 mediated lysis of the host.<sup>[21]</sup>

439 Previous publications have reported phage densities utilized for effective bacterial treatments:  
440 shouldn't be too low, less than  $10^7$  PFU/cm<sup>3</sup>, because there won't be enough phage particles to  
441 lyse enough of their host growing in logarithmic phase;<sup>[26, 27]</sup> and shouldn't be too high, higher  
442 than  $10^8$  PFU/cm<sup>3</sup>, which often results in poor pharmacodynamic effects.<sup>[26, 27]</sup>

443 According to our study we can say computer models coupled with *in vitro* testing are indicative  
444 that predicted optimal dose is consistent with the behavior of the infection curves that have been  
445 previously reported. <sup>[21, 26, 27]</sup>

446

#### 447 4. CONCLUSIONS

448 The mathematical modeling of viral infections in *P. aeruginosa* allowed us to analyze the  
449 dynamics and kinetics of our phage-host system. The combined use of deterministic and  
450 stochastic kinetics helped us to elucidate the evolution of the population with two frameworks:  
451 the law of mass action and stochastic kinetics. The optimal dose predicted for phage F1  
452 effectively reduced bacterial populations, and it also was applied to other two other phages (F2  
453 and F3); which indicates that our models can describe different phage-host systems. The optimal  
454 dose is in the range of effectiveness reported, which was in the range of  $10^7$ - $10^8$ . Our results  
455 validate that phage therapy is a viable alternative to control *P. aeruginosa* and with appropriate  
456 mathematical modeling the behavior of the phage-host interaction can be predicted. Our data was  
457 shown to be effective using a single phage type and a future project our group should study is the  
458 behavior of a system using phage cocktails to delay the appearance of phage-resistant cells.

459

460

461

462

463 **6. ACKNOWLEDGEMENTS**

464 We wish to thank Zachary Hobbs, Research Associate of the T4 Bacteriophage Lab at The  
465 Evergreen State College, Olympia, WA, USA, for his valuable comments and edits to this  
466 manuscript.

467 This work was supported by Universidad de los Andes under the interfaculty grant “Programa de  
468 consolidación de la interacción entre las Facultades de Ciencias e Ingeniería, Bioprospección de  
469 microorganismos y análisis de su aplicación por medio de técnicas de modelamiento”, 2007.

470

471 **REFERENCES**

472

- 473 [1] J. W. Costerton, *Science*. **1999**, 284, 1318.
- 474 [2] K. Poole, K. Krebs, C. McNally, and S. Neshat, *J. Bacteriol.* **1993**, 175, 22.
- 475 [3] M. H. Kollef, and V. J. Fraser, *Ann. Intern. Med.* **2001**, 134, 4.
- 476 [4] W. C. Summers, *Annu. Rev. Microbiol.* **2001**, 55, 1.
- 477 [5] J. Azeredo, and I. W. Sutherland, *Curr. Pharm. Biotechnol.* **2008**, 9, 4.
- 478 [6] M. Skurnik, and E. Strauch, *Int. J. Med. Microbio.* **2006**, 296, 1.
- 479 [7] Y. Lebeque Pérez, H. J. Morris Quevedo, and N. Calás Viamonte, *Rev. Cubana Med.* **2006**, 45, 1.
- 480 [8] E. L. P. Rojas, D. P. de León Pandolfí, and R. R. Ponce, *Acta Méd. Peruana.* **2008**, 25, 3.
- 481 [9] D. C. Ardila, M. Vives-Florez, and A. F. G. Barrios, *Proceedings 8th congress of chemical engineering.*  
482 **2009**, 1, 1.
- 483 [10] A. Arkin, J. Ross, and H. H. McAdams, *Genetics.* **1998**, 149, 4.
- 484 [11] A. F. Gonzalez Barrios, and L. E. K. Achenie, *Biosystems.* **2010**, 99, 1.
- 485 [12] R. Jain, A. L. Knorr, J. Bernacki, and R. Srivastava, *Biotechnol. Progr.* **2006**, 22, 6.
- 486 [13] D. T. Gillespie, *J. Phys. Chem.* **1977**, 81, 25.
- 487 [14] S. J. Labrie, J. E. Samson, and S. Moineau, *Nature Rev. Microbiol.* **2010**, 8, 5.
- 488 [15] A. F. González, V. Covo, L. M. Medina, M. Vives-Florez, and L. Achenie, *Bioprocess Biosyst. Eng.* **2009**,  
489 32, 4.

- 490 [16] B. J. Cairns, A. R. Timms, V. A. A. Jansen, I. F. Connerton, R. J. H. Payne, *PLoS Pathog.* **2009**, 5,1.
- 491 [17] X. Bardina, D. Bascompte, D. Rovira, S. Tindell. *arXiv.* **2011**
- 492 [18] H. Schmidt, and M. Jirstrand, *Bioinformatics.* **2005**, 22, 4.
- 493 [19] O. Chis, J. R. Banga, E. Balsa-canto, *Bioinformatics.* **2011**, 27, 18
- 494 [20] M. Villamizar, H. Castro, and A. F. Gonzalez Barrios, *Proceedings Of The First Eela-2 Conference.* **2009**,
- 495 1, 1.
- 496 [21] A. Curtright, and S. Abedon, *J. Bioanal. Biomed.* **2001**, 6, 2.
- 497 [22] R. J. Payne, and V. A. Jansen, *J. Theor. Biol.* **2001**, 208, 1.
- 498 [23] R. J. Payne, and V. A. Jansen, *Clin. Pharmacol. Ther.* **2000**, 68, 3.
- 499 [24] S. T. Abedon. *Bacteriophage*, **2011**, 1, 1.
- 500 [25] C. K. Mathews, E. M. Kutter, G. Mosig, P. B. Berget, *Bacteriophage T4*. 1st edition, American Society for
- 501 Microbiology, Washington D. C, **1993**.
- 502 [26] S. T. Abedon, and C. Thomas-Abedon, *Curr. Pharm. Biotechnol.* 2010, 11, 1.
- 503 [27] S. T. Abedon. *Adv. Appl. Microbiol.* **2011**, 77.

504

505

506

507

508

509

510

511

512

513

514

515

516

517

### Figure captions

518 **Figure 1.** Global petri net for *P. aeruginosa* P1, P3 and P4 merged model.  $K_{ab}$  represents the  
519 kinetic parameter  $a$  for strain  $b$  (e.g.,  $K_{31}$  means kinetic parameter  $K_3$  for *P. aeruginosa* P1).  $x_a$   
520 and  $y_a$  means uninfected and infected cells for strain  $a$  respectively. (e.g.,  $x_1$  uninfected cells for  
521 *P. aeruginosa* P1 and  $y_1$  is infected cells for *P. aeruginosa* P1). Circles and rectangles represent  
522 coins and transitions respectively.

523 **Figure 2.** Model predictions in comparison with experimental data for uninfected cells of *P.*  
524 *aeruginosa* P1 (A), *P. aeruginosa* P3 (B), *P. aeruginosa* P4 (C). The infections were performed  
525 with phage F1.

526 **Figure 3.** Total uninfected cells profile obtained by the simulation for the merge model mixing  
527 *P. aeruginosa* P1, P3 and P4 strains. Optimal dose of phage F1 was used to achieve infection.

528 **Figure 4.** Uninfected cells profile for the merged model (*P. aeruginosa* P1, P3, and P4) based on  
529 the stochastic kinetics model. Mean and standard deviation was calculated from 100 000 runs.

530 **Figure 5.** Challenge test with a dose above and below the optimal dose predicted. *P. aeruginosa*  
531 P4 infected with a dose of  $10^6$  PFU/cm<sup>3</sup> of phage F1 compared with the positive control (P4  
532 without any phage) (A). *P. aeruginosa* P4 infected with a dose of  $10^8$  PFU/cm<sup>3</sup> of phage F1  
533 compared with the positive control (P4 without any phage) (B).

534 **Nomenclature:**

535 **F1** Phage F1

536 **F2** Phage F2

537 **F3** Phage F3



- 538  $k_1$  Infection rate ( $\text{min} \cdot \text{phage particles}/\text{cm}^3$ )<sup>-1</sup>
- 539  $k_2$  Death rate of uninfected cells ( $\text{min}$ )<sup>-1</sup>
- 540  $k_3$  Rate of lysis of infected cells ( $\text{min}$ )<sup>-1</sup>
- 541  $k_4$  Rate at which the phage progeny was produced ( $\text{PFU}/\text{cell min}$ )
- 542  $k_5$  Rate at which the free phage particles were degraded ( $\text{min}$ )<sup>-1</sup>
- 543  $k_6$  Dead rate of resistant cells ( $\text{min}$ )<sup>-1</sup>
- 544  $K_{s,R}$  Monod constant for uninfected cells resistant to the phage ( $\text{mol}/\text{m}^3$  glucose)
- 545  $K_{s,x}$  Monod constant for uninfected cells ( $\text{mol}/\text{m}^3$  glucose)
- 546  $K_{s,y}$  Monod constant for infected cells ( $\text{mol}/\text{m}^3$  glucose)
- 547  $K_{s,z}$  Monod constant for uninfected cells nonresistant to the phage ( $\text{mol}/\text{m}^3$  glucose)
- 548 **P1** *Pseudomonas aeruginosa* P1
- 549 **P3** *Pseudomonas aeruginosa* P3
- 550 **P4** *Pseudomonas aeruginosa* P4
- 551 **P** Free phage density ( $\text{PFU}/\text{cm}^3$ )
- 552 **PD** Initial phage dose ( $\text{PFU}/\text{cm}^3$ )
- 553 **R** Uninfected cells resistant to the phage ( $\text{CFU}/\text{cm}^3$ )
- 554 **s** Substrate density ( $\text{mol}/\text{m}^3$ )

- 555  $t_i$  Time where the bacterial population is minimized (*min*)
- 556  $U$  Step function.  $U$  is 0 when  $t \leq 480$  min and 1 when  $t > 480$ min  
557
- 558  $x$  Uninfected cell density ( $CFU/cm^3$ )
- 559  $x_I$  cell population of P1 at  $t_i$  ( $CFU/cm^3$ )
- 560  $x_3$  cell population of P3 at  $t_i$  ( $CFU/cm^3$ )
- 561  $x_4$  cell population of P4 at  $t_i$  ( $CFU/cm^3$ )
- 562  $x_{p1(0)}$  Initial condition of living cells for *P. aeruginosa* P1 ( $CFU/cm^3$ )
- 563  $x_{p3(0)}$  Initial condition of living cells for *P. aeruginosa* P3 ( $CFU/cm^3$ )
- 564  $x_{p4(0)}$  Initial condition of living cells for *P. aeruginosa* P4 ( $CFU/cm^3$ )
- 565  $y$  Infected cell density ( $CFU/cm^3$ )
- 566  $y_{R/s}$  Yield factor relating production of uninfected cells resistant to the phage, to substrate  
567 consumed ( $CFU/grams$  of glucose)
- 568  $y_{x/s}$  Yield factor relating production of uninfected bacterial cells to substrate consumed  
569 ( $CFU/grams$  of glucose)
- 570  $y_{y/s}$  Yield factor relating production of infected bacterial cells to substrate consumed  
571 ( $CFU/grams$  of glucose)
- 572  $y_{z/s}$  Yield factor relating production of uninfected cells nonresistant to the phage, to substrate  
573 consumed ( $CFU/grams$  of glucose)

574  $z$  Uninfected cells nonresistant to de phage ( $CFU/cm^3$ )

575

576 **Greek symbols**

577  $\mu_{max,R}$  Maximal growth of uninfected cells resistant to the phage ( $min^{-1}$ )

578  $\mu_{max,x}$  Maximal growth of uninfected cells ( $min^{-1}$ )

579  $\mu_{max,y}$  Maximal growth of infected cells ( $min^{-1}$ )

580  $\mu_{max,z}$  Maximal growth of uninfected cells nonresistant to the phage ( $min^{-1}$ )

581  $\mu_R$  Growth rate of uninfected cells resistant to the phage ( $min^{-1}$ )

582  $\mu_x$  Growth rate of uninfected cells ( $min^{-1}$ )

583  $\mu_y$  Growth rate of infected cells ( $min^{-1}$ )

584  $\mu_z$  Growth rate of uninfected cells nonresistant to the phage ( $min^{-1}$ )

585

**Table 1** (on next page)

Table 1. Experimental- simulation fitness evaluation for each *P. aeruginosa* strain organized from the best fit to the worst fit for each strain.

1 **Table 1.** Experimental- simulation fitness evaluation for each *P. aeruginosa* strain organized from the best fit to the worst fit for each strain.

<i>P1</i>		<i>P3</i>		<i>P4</i>	
Model	Squares sum	Model	Squares sum	Model	Squares sum
6	$1.01 \times 10^{10}$	6	$2.69 \times 10^{17}$	2	$4.19 \times 10^{16}$
3	$1.74 \times 10^{10}$	2	$3.37 \times 10^{17}$	1	$7.94 \times 10^{16}$
1	$1.77 \times 10^{10}$	1	$4.62 \times 10^{17}$	5	$1.32 \times 10^{17}$
2	$1.85 \times 10^{10}$	3	$4.85 \times 10^{17}$	3	$4.17 \times 10^{17}$
5	$2.26 \times 10^{10}$	5	$9.21 \times 10^{18}$	6	$5.85 \times 10^{17}$
4	$2.8 \times 10^{10}$	4	$9.53 \times 10^{18}$	4	$1.40 \times 10^{19}$

2

**Table 2** (on next page)

Table 2. Kinetic parameters for the best fit deterministic phage-strain models for *P. aeruginosa* P1, P3 and P4

1

2 **Table 2.** Kinetic parameters for the best fit deterministic phage-strain models for *P. aeruginosa* P1, P3  
3 and P4

<i>Parameter</i>	<i>P1</i>	<i>P3</i>	<i>P4</i>
	Model six	Model six	Model two
$k_1$ ( $\text{min} \cdot \text{phage particles/cm}^3$ ) <sup>-1</sup>	1.000 65	1	1.5
$k_2$ ( $\text{min}$ ) <sup>-1</sup>	0	0	0
$k_3$ ( $\text{min}$ ) <sup>-1</sup>	0.01	0.01	0.01
$k_4$ (PFU/cell x min)	0.16	0.16	0.16
$k_5$ ( $\text{min}$ ) <sup>-1</sup>	0	0	0
$k_6$ ( $\text{min}$ ) <sup>-1</sup>	0	0	0
$K_{s,x}$ ( $\text{mol/m}^3$ glucose)	0.007	0.007	1
$K_{s,y}$ ( $\text{mol/m}^3$ glucose)	10	10	14.99
$Y_{x/s}$ (cells/grams of glucose)	20 001.1	257 877	257 877
$Y_{y/s}$ (cells/grams of glucose)	969 000	688 938	688 938
$\mu_{\max,x}$ ( $\text{min}^{-1}$ )	0.004	0.016	0.003
$\mu_{\max,y}$ ( $\text{min}^{-1}$ )	0.001	0.002	0.005

4

**Table 3** (on next page)

Comparison between the results in the reduction of *Pseudomonas aeruginosa* P1, P3, and P4 strains population in the simulation and in the experimental validation at time point 1100 min. The total population reduction was calculated as the difference



1 **Table 3.** Comparison between the results in the reduction of *Pseudomonas aeruginosa* P1, P3,  
 2 and P4 strains population in the simulation and in the experimental validation at time point 1100  
 3 min. The total population reduction was calculated as the difference between the total  
 4 population of the control curve (cells growing without phage infection) at 1100min and the total  
 5 population of the infection curve at 1100 min

<i>Strain</i>	<i>Total population reduction (CFU/cm<sup>3</sup>) in simulation results</i>	<i>Total population reduction (CFU/cm<sup>3</sup>) in experimental validation results</i>	<i>Difference in order of magnitude between results</i>
P1	1.19 x 10 <sup>5</sup>	2.95 x 10 <sup>6</sup>	1
P3	5 x 10 <sup>8</sup>	1.17 x 10 <sup>8</sup>	0
P4	9 x 10 <sup>6</sup>	3.17 x 10 <sup>7</sup>	1

6

**Table 4**(on next page)

Table 4. Total population reduction of *Pseudomonas aeruginosa* P1, P3 and P4 with phages F2 and F3 (Optimal dose extrapolation) at time point 1100 min. The total population reduction was calculated as the difference between the total population of th

1

2 **Table 4.** Total population reduction of *Pseudomonas aeruginosa* P1, P3 and P4 with phages F2  
3 and F3 (Optimal dose extrapolation) at time point 1100 min. The total population reduction was  
4 calculated as the difference between the total population of the control curve (cells growing  
5 without phage infection) at 1100min and the total population of the infection curve at 1100 min

6

<i>Strain</i>	<i>Phage</i>	<i>Total population reduction (CFU/cm<sup>3</sup>)</i>
P1	F2	$5.03 \times 10^7$
	F3	$4.51 \times 10^7$
P3	F2	$4.85 \times 10^8$
	F3	$3.15 \times 10^9$
P4	F2	$4.41 \times 10^8$
	F3	$6.7 \times 10^8$

7

8

9

# Figure 1

Global petri net for *P. aeruginosa* P1, P3 and P4 merged model.  $K_{ab}$  represents the kinetic parameter  $a$  for strain  $b$  (e.g.,  $K_{31}$  means kinetic parameter  $K_3$  for *P. aeruginosa* P1).  $x_a$  and  $y_a$  means uninfected and infected

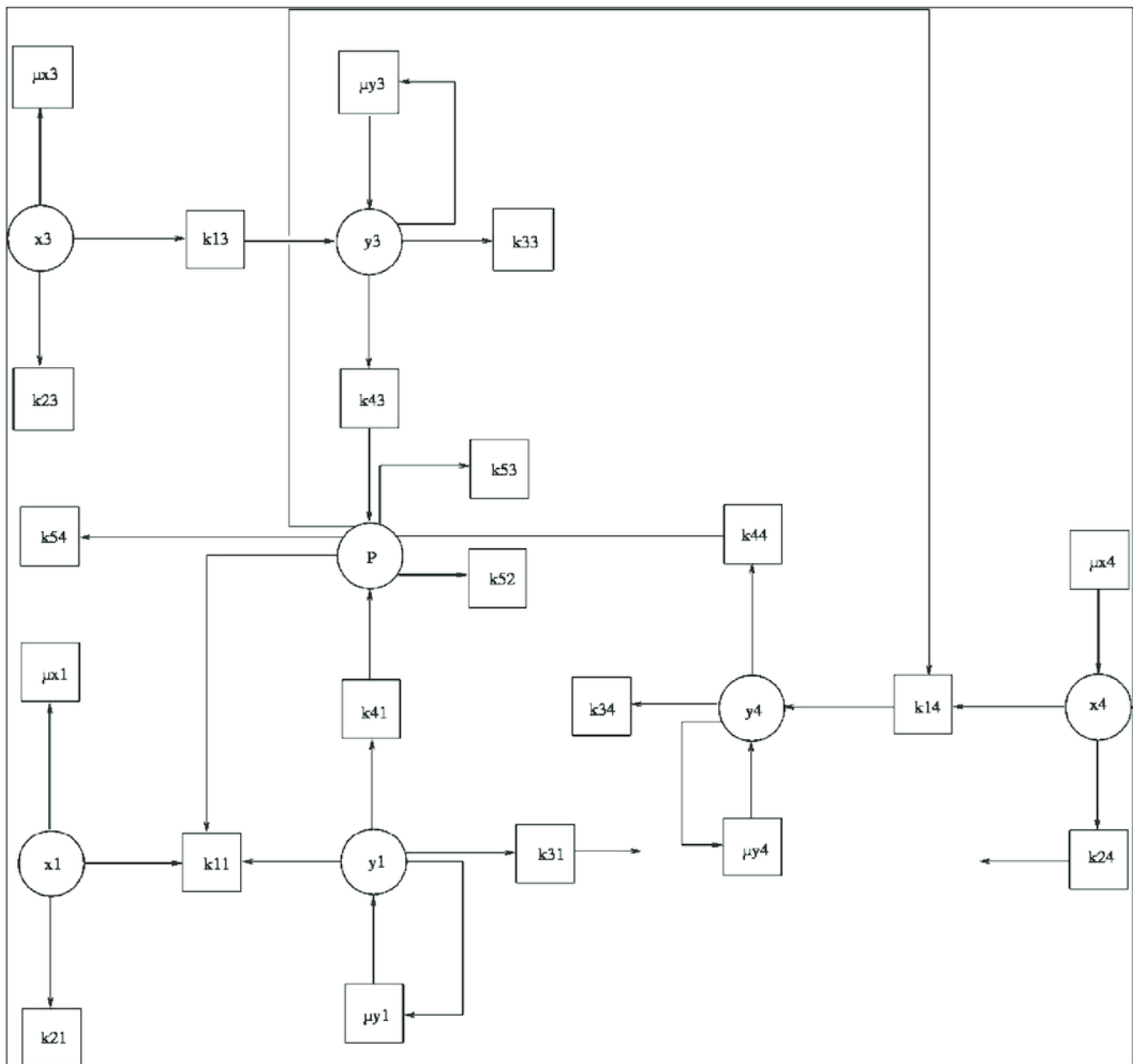


## Figure 2

Model predictions in comparison with experimental data for uninfected cells of *P. aeruginosa* P1 (A), *P. aeruginosa* P3 (B), *P. aeruginosa* P4 (C). The infections were performed with phage F1.

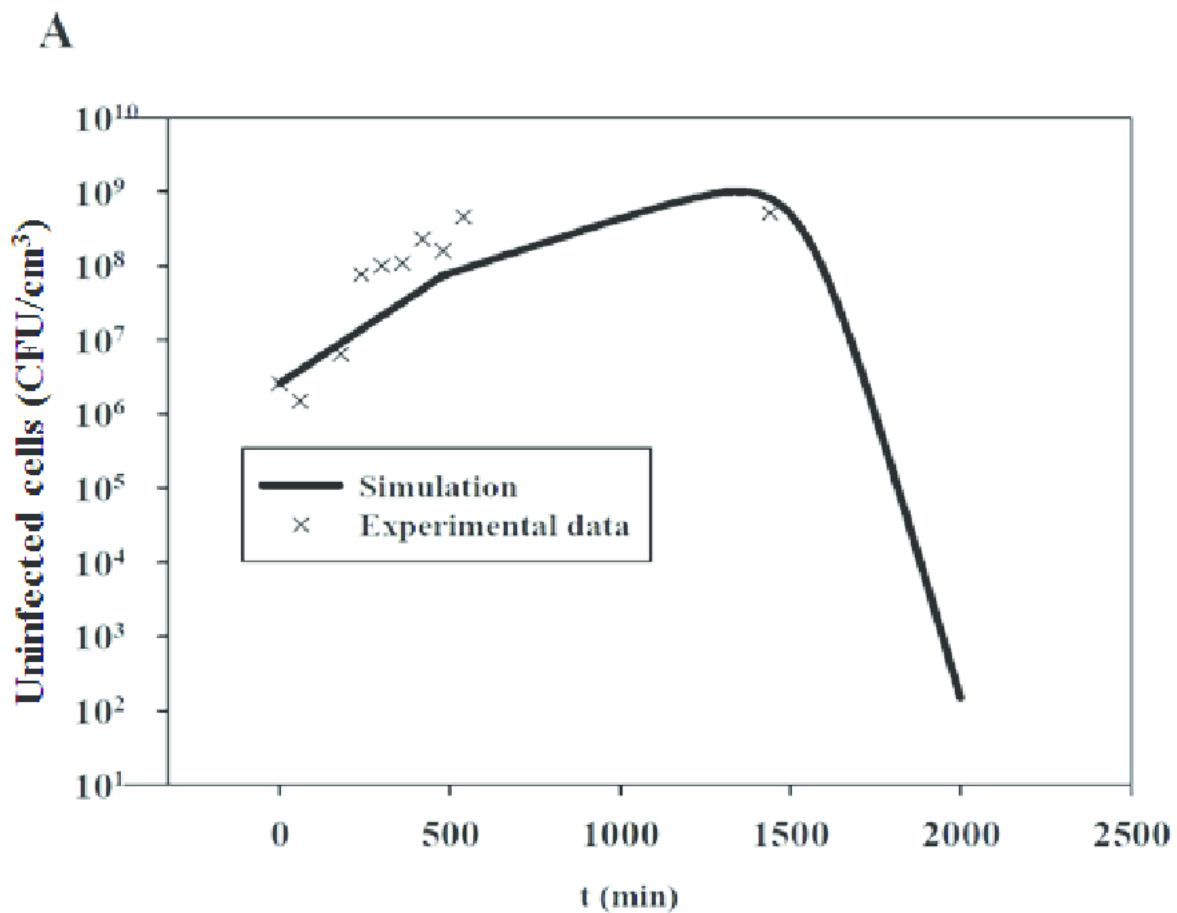


## Figure 3

Model predictions in comparison with experimental data for uninfected cells of *P. aeruginosa* P1 (A), *P. aeruginosa* P3 (B), *P. aeruginosa* P4 (C). The infections were performed with phage F1.

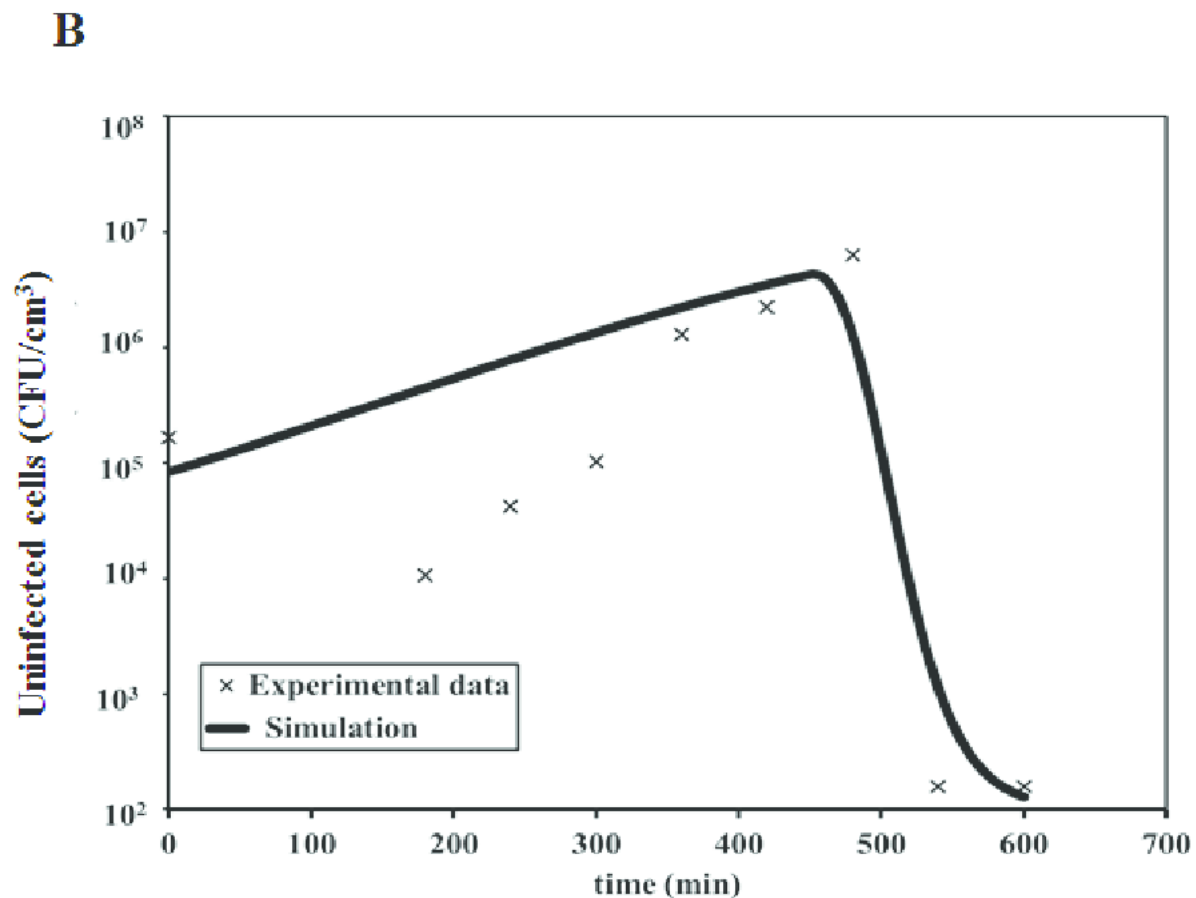


## Figure 4

Model predictions in comparison with experimental data for uninfected cells of *P. aeruginosa* P1 (A), *P. aeruginosa* P3 (B), *P. aeruginosa* P4 (C). The infections were performed with phage F1.

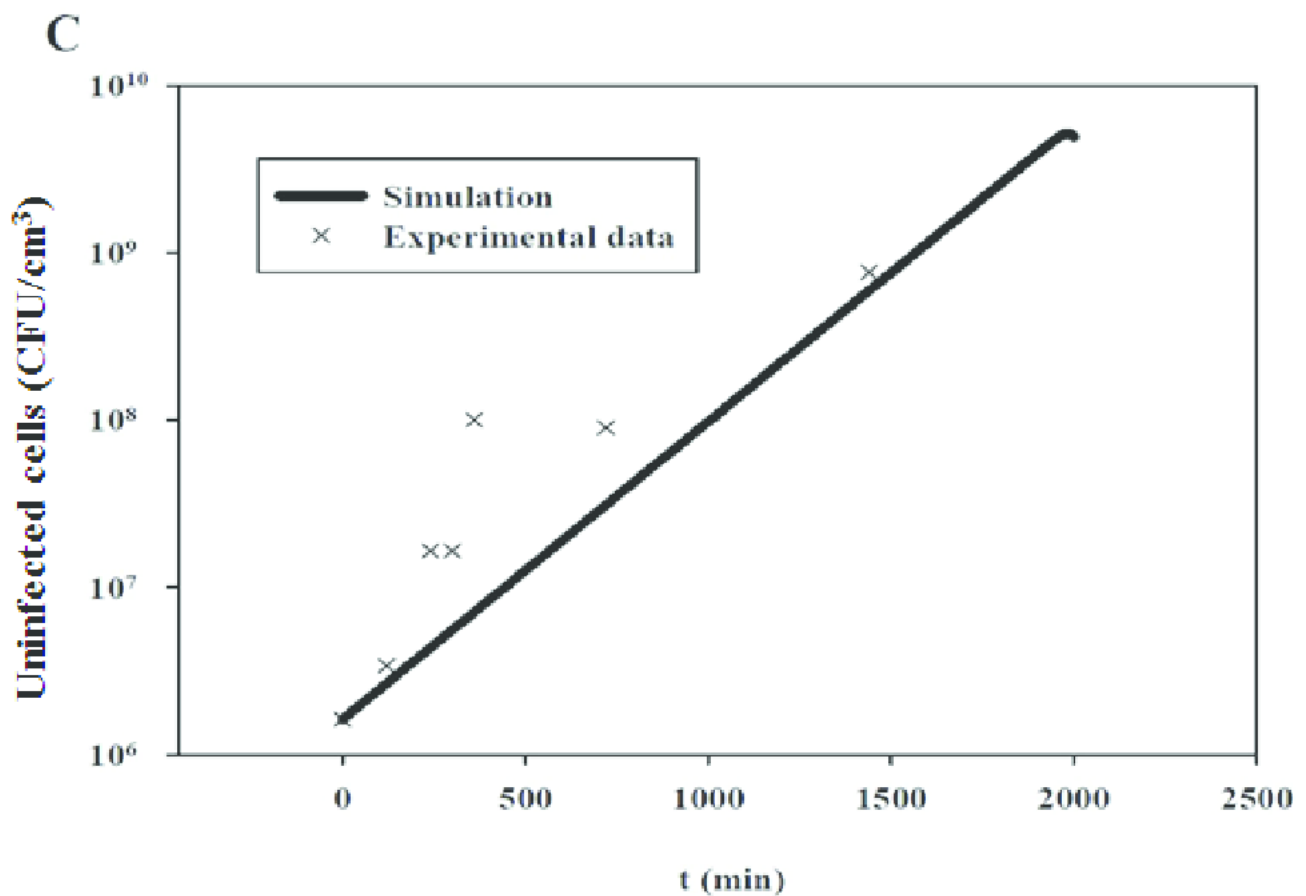


## Figure 5

Total uninfected cells profile obtained by the simulation for the merge model mixing *P. aeruginosa* P1, P3 and P4 strains. Optimal dose of phage F1 was used to achieve infection.

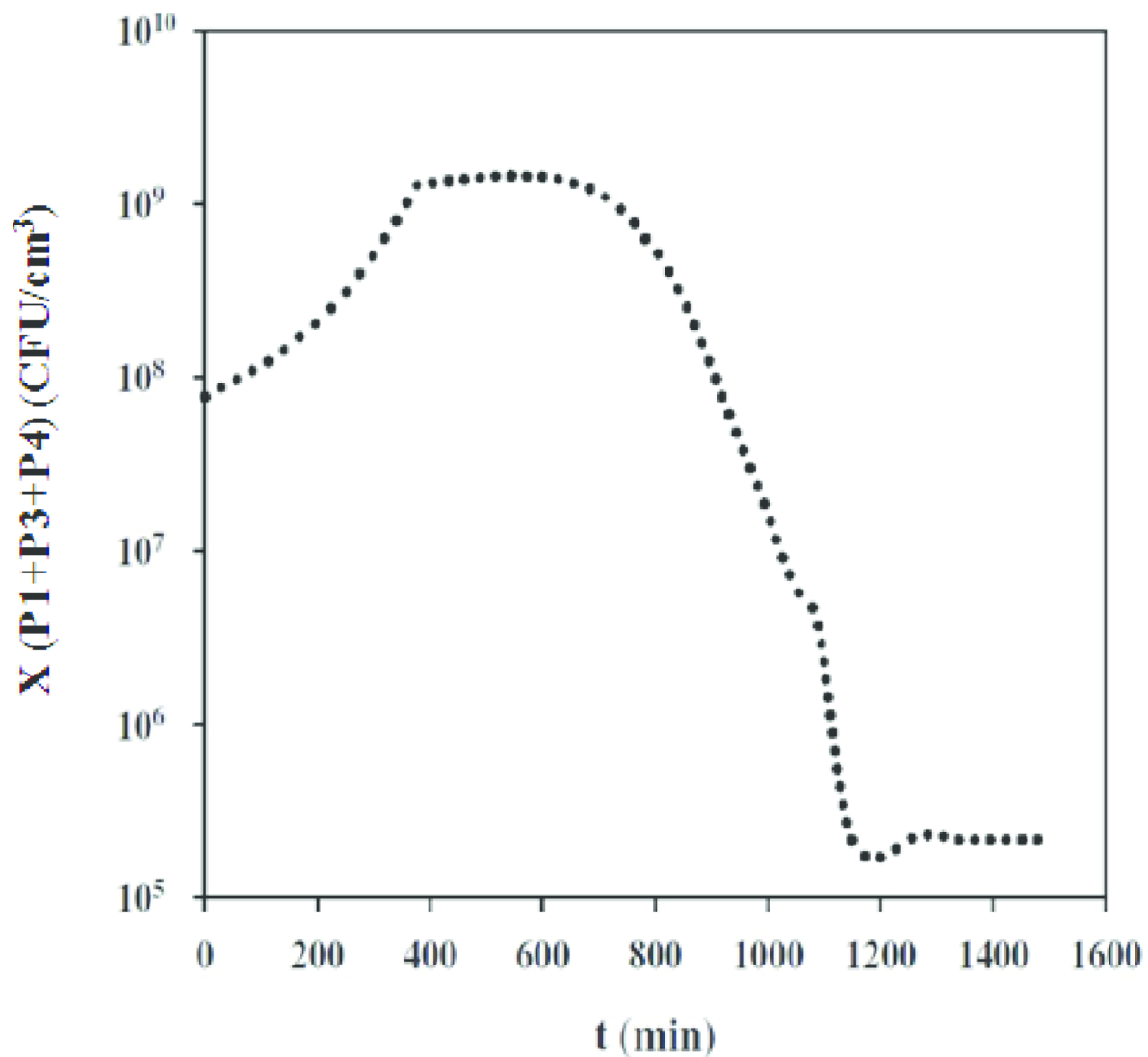




## Figure 6

Uninfected cells profile for the merged model (*P. aeruginosa* P1, P3, and P4) based on the stochastic kinetics model. Mean and standard deviation was calculated from 100 000 runs.

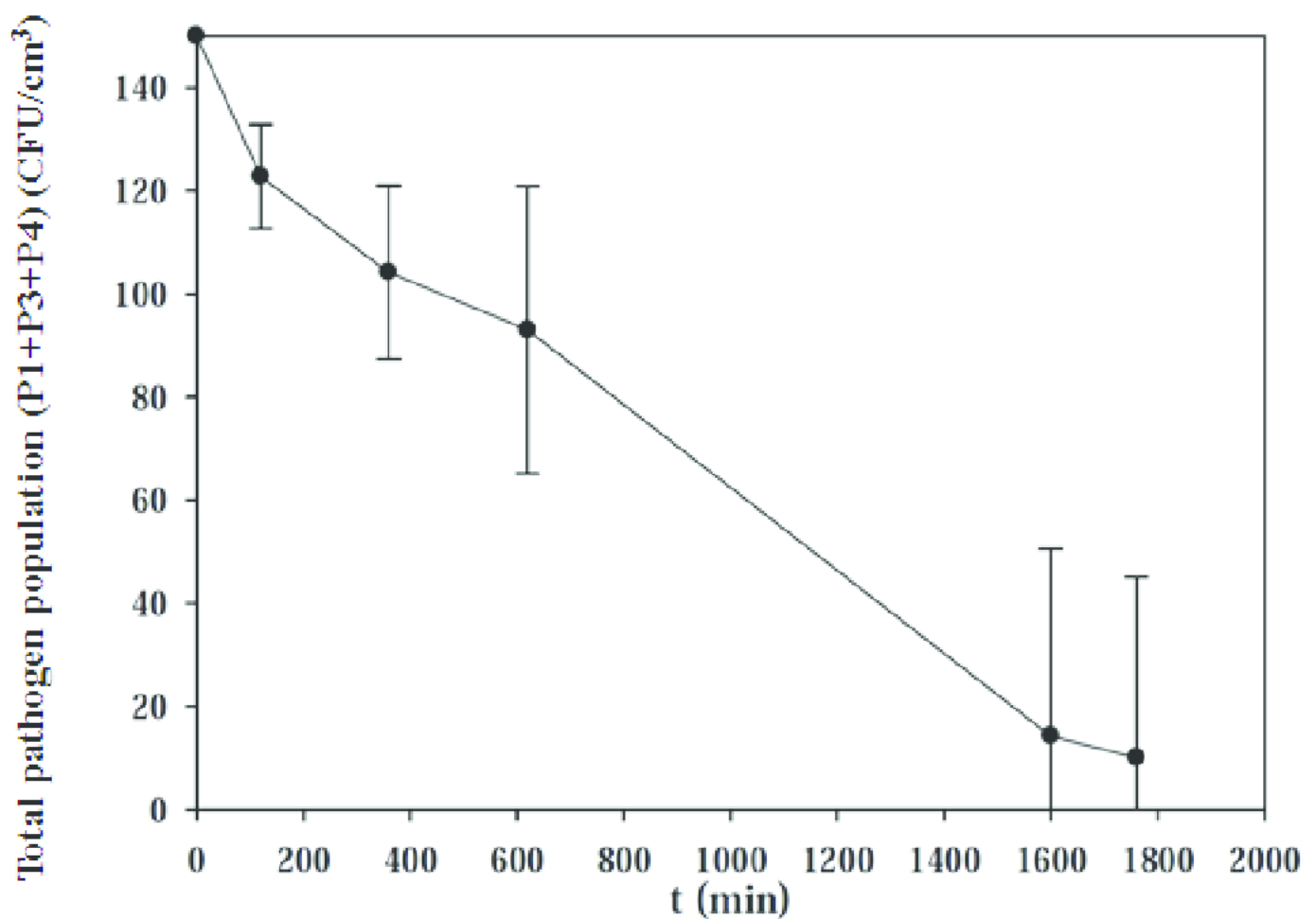


## Figure 7

Challenge test with a dose above and below the optimal dose predicted. *P. aeruginosa* P4 infected with a dose of  $10^6$  PFU/cm<sup>3</sup> of phage F1 compared with the positive control (P4 without any phage) (A). *P. aeruginosa* P4 infected

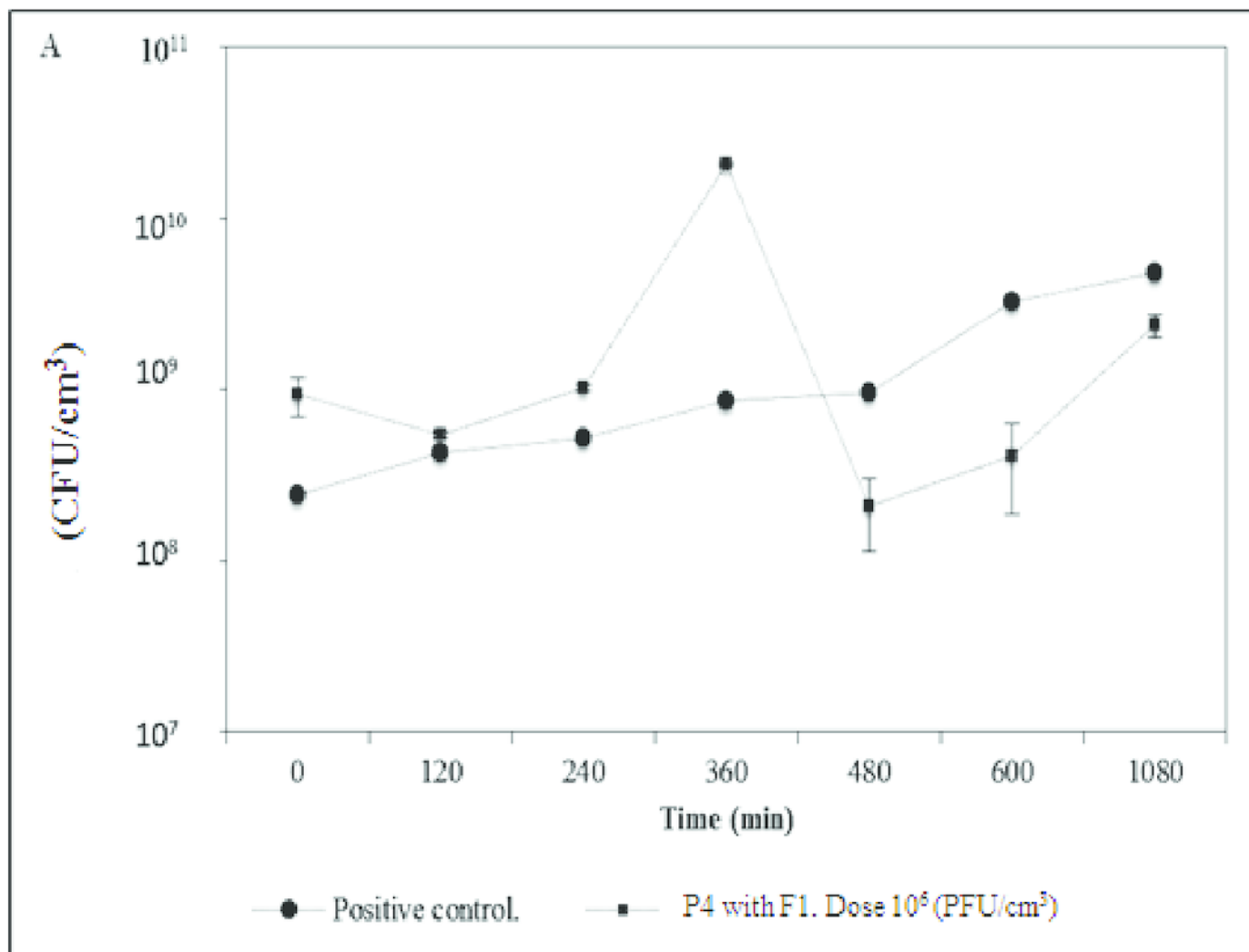


## Figure 8

Challenge test with a dose above and below the optimal dose predicted. *P. aeruginosa* P4 infected with a dose of  $10^6$  PFU/cm<sup>3</sup> of phage F1 compared with the positive control (P4 without any phage) (A). *P. aeruginosa* P4 infected

